

# The role of heavy quarks in light hadron fragmentation.

Manuel Epele\* and Carlos García Canal†

*Instituto de Física La Plata, UNLP, CONICET Departamento de Física,  
Facultad de Ciencias Exactas, Universidad de La Plata, C.C. 69, La Plata, Argentina*

R. Sassot‡

*Departamento de Física and IFIBA, Facultad de Ciencias Exactas y Naturales,  
Universidad de Buenos Aires, Ciudad Universitaria, Pabellón 1 (1428) Buenos Aires, Argentina*

We investigate the role of heavy quarks in the production of light flavored hadrons and in the determination of the corresponding non perturbative hadronization probabilities. We define a general mass variable flavor number scheme for fragmentation functions that accounts for heavy quark mass effects, and perform a global QCD analysis to an up-to-date data set including very precise Belle and BaBar results. We show that the mass dependent picture provides a much more accurate and consistent description of data.

PACS numbers: 13.87.Fh, 13.85.Ni, 12.38.Bx

*Introduction.*— The effects of heavy quark masses in hard processes and the appropriate definition of parton probability densities for such species of quarks have been very actively studied in recent years [1]. When a heavy quark participates in a hard process, and the characteristic energy of the process under consideration is not far from the heavy quark mass scale, the most natural choice is to treat these particles as massive throughout the calculation, rather than appeal to the more conventional massless parton approximation. However, when the scale of the process exceeds by large the mass scale of the heavy quarks, mass corrections not only become negligible, but the all-order resummations implicit in massless parton approaches become crucial. This situation clearly represents a challenge for a precise and consistent comparison of processes occurring at very different energy scales, as it necessarily happens in a global QCD analysis designed to extract non-perturbative parton distribution functions (PDFs) [2] or fragmentation functions (FFs) [3, 4] from the data. To overcome this problem, in most modern global QCD analysis of data, the so called general mass variable flavor number (GMVFN) schemes [5–8] for parton densities are introduced, as they allow to retain the advantages of massive schemes near the mass thresholds and those of the massless approach at high energies, smoothly interpolating between both regimes.

In fact, different GMVFN approaches have been applied to the analysis of fragmentation probabilities of heavy quarks into heavy flavored hadrons [9–11], but until now little attention has been paid in this respect to light hadron fragmentation processes. Since the charm and bottom content in the proton is rather limited, the production of light mesons via heavy quarks of course is strongly suppressed relative to that via light quarks both

in proton-proton collisions and in semi-inclusive deep elastic scattering (SIDIS). Heavy quark corrections are thus expected to be negligible for these processes. But that is not the case for single inclusive electron-positron annihilation (SIA) into light mesons, where the charm and bottom contribution to the cross section is estimated to be comparable in size to that of the light flavors [12]. Whereas charm and bottom mass corrections may still be negligible in SIA experiments tuned at the mass of the Z boson, they are certainly relevant at the energy scales of the more recent BaBar and Belle experiments [13, 14], which are just above the bottom mass threshold.

In this paper we compute the single inclusive electron-positron annihilation cross section with non zero masses for the charm and bottom quarks at first order in the strong coupling constant  $\alpha_s$ , and we estimate the effects of retaining these mass corrections in pion production. Since we find the mass dependence to be large but we want to keep the advantages of the NLO massless approximation at high energies, we define a general mass variable flavor number scheme for fragmentation functions in the lines of the FONLL scheme [15, 16], commonly used for PDFs. We implement numerically this scheme in Mellin moment space for the fast computation of the cross sections as required by QCD global analyses, and we perform them including recent Belle and BaBar data. The mass dependent picture introduced by the GMVFN scheme is found to be relevant in the extraction of fragmentation functions both in terms of the quality of the fit to data and in the reduction of the normalization shifts applied to data that are customarily included in global fits. The shape of the charm into pion fragmentation function, that contributes significantly to the cross section at the energies of the Belle and BaBar experiments, is noticeably modified relative to the results obtained within a massless scheme. The bottom fragmentation, constrained mainly by higher energy data, remains similar to the one found in the massless approximation.

*Factorization Schemes.*— Most analyses of quark fragmentation into light flavored hadrons [3, 4] rely on

\*Electronic address: manuepele@fisica.unlp.edu.ar

†Electronic address: garcia@fisica.unlp.edu.ar

‡Electronic address: sassot@df.uba.ar

the massless perturbative QCD approximation, supplemented with heavy quark mass thresholds, where the corresponding heavy quarks become active, contribute to cross sections and enter the scale or evolution equations [17]. This zero mass variable flavor number (ZMVFN) scheme is the simplest framework to compute the SIA cross section [18]:

$$\frac{d\sigma^{\text{ZMVFN}}}{dz} = \sum_{i=q,g,h} \hat{\sigma}_i^{\text{ZM}}(z, Q) \otimes D_i^{\text{ZM}}(z, Q) \quad (1)$$

where  $\hat{\sigma}_i^{\text{ZM}}$  is the massless partonic SIA cross section into a parton of flavor  $i$ , and  $D_i^{\text{ZM}}$  are the corresponding FFs, for which we omit in what follows the dependence on the scaled hadron energy fraction  $z$ .  $\otimes$  represent the appropriate convolution over  $z$ , and  $Q$  is the center of mass energy.  $D_i^{\text{ZM}}$  evolves in the scale  $Q$  through massless QCD evolution equations for any parton flavor  $i$ , that include light ( $q$ ) and heavy ( $h$ ) quarks and antiquarks and gluons ( $g$ ). Eq.(1) gives a remarkably good approximation at NLO and NNLO well above mass threshold  $m_h$  [12, 19], i.e.  $Q \gg m_h$ , but fails to account for mass effects. Alternatively, in a massive scheme (M), heavy quark masses are kept at the partonic cross section level,

$$\frac{d\sigma^{\text{M}}}{dz} = \sum_{i=q,g} \hat{\sigma}_i^{\text{M}}(Q, m_h) \otimes D_i^{\text{M}}(Q) + \hat{\sigma}_h^{\text{M}}(Q, m_h) \otimes D_h^{\text{M}} \quad (2)$$

the light flavored FFs  $D_{q,g}^{\text{M}}(Q)$  still evolve through massless QCD evolution equations in NLO, although heavy quark loops contribute above  $\mathcal{O}(\alpha_S^2)$ , and heavy quark FFs  $D_h^{\text{M}}$  decouple from the QCD evolution [20]. The massive scheme gives a good description near the mass thresholds, but fail to converge to the massless limit at high energies because of potentially large logarithmic contributions ( $\alpha_S^k \log^k(m_h/Q)$ ) present in the partonic cross sections  $\hat{\sigma}_i^{\text{M}}$  that spoil the convergence of the perturbation expansion. These logarithmic contributions are effectively resummed in the renormalization group improved ZM approximation. In fact, it has been shown [21] that in the massless limit, i.e.  $Q \gg m_h$ ,

$$\hat{\sigma}_i^{\text{M}}(Q, m_h) \xrightarrow{m_h \rightarrow 0} \sum_{j=q,g,h} \hat{\sigma}_j^{\text{ZM}}(Q) \otimes \mathcal{A}_{ji}(Q/m_h) \quad (3)$$

where all logarithmic contributions can be factorized in an operator matrix  $\mathcal{A}_{ij}$  that is independent of the hard process under consideration [10, 11, 22].

The advantages of both the zero mass and the massive schemes can be exploited in a general mass (GM) scheme, which defines the corresponding fragmentation probabilities through

$$\frac{d\sigma^{\text{GMVFN}}}{dz} = \sum_{i=q,g,h} \hat{\sigma}_i^{\text{GM}}(Q, m_h) \otimes D_i^{\text{GM}}(Q) \quad (4)$$

where a subtracted massive partonic cross section

$$\hat{\sigma}_j^{\text{GM}}(Q, m_h) = \sum_{i=q,g,h} \hat{\sigma}_i^{\text{M}}(Q, m_h) \otimes \mathcal{A}_{ij}^{-1}(Q/m_h) \quad (5)$$

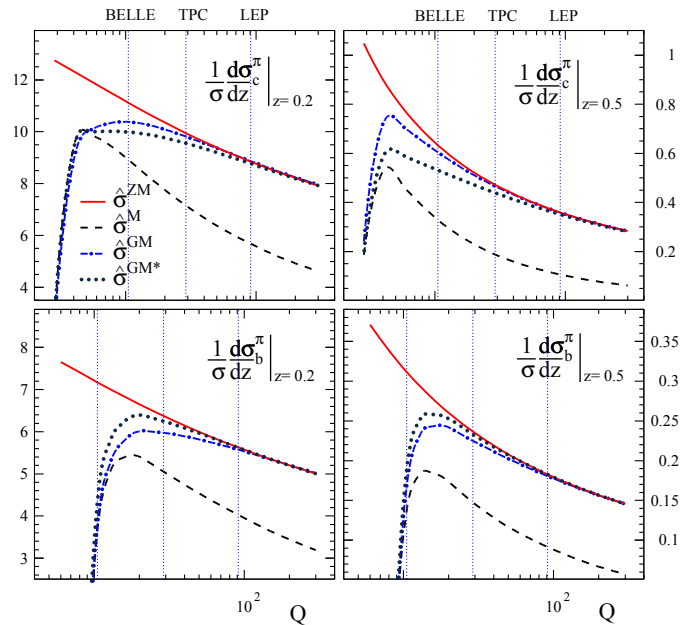


FIG. 1: Charm and bottom contribution to the SIA cross section computed with different approximations for the partonic cross sections and the same set of FFs.

guarantees the correct massless behavior at high energies. The fragmentation functions  $D_j^{\text{GM}}(Q)$  obey standard evolution equations as in the ZM scheme and the continuity across the thresholds can be ensured by imposing the following matching condition

$$D_j^{\text{GM}}(m_h) = \sum_{i=q,g,h} \mathcal{A}_{ji}(1) \otimes D_i^{\text{M}}(m_h) \quad (6)$$

analogously as in the FONLL scheme for PDFs [15, 16].

In order to illustrate the effects arising from the use of the different approximations for the partonic cross sections, in Fig.1 we show the charm and bottom contribution to the SIA pion cross section (upper and lower panels, respectively) as a function of the center of mass energy  $Q$  at two reference values of  $z$ . For the comparison, the same set of NLO FFs that will be described in detail in the next section, is convoluted with the NLO massless (ZM) partonic cross section (red solid lines), the full  $\mathcal{O}(\alpha_S)$  massive (M) result (black dashed lines), and the subtracted (GM) approximation (blue dot-dashed lines). Even though the scheme defined by Eqs.(4-6) interpolates between the massive behavior near thresholds and the desired zero mass limit at  $Q \gg m_h$ , this solution is clearly not unique. The same limits can be satisfied in alternative factorization schemes where the convergence to the massless limit happens at a lower or higher energy scale. For instance, substituting

$$\hat{\sigma}_j^{\text{GM}} \longrightarrow \hat{\sigma}_j^{\text{GM}*} = (1 - f(Q)) \hat{\sigma}_j^{\text{M}} + f(Q) \hat{\sigma}_j^{\text{GM}} \quad (7)$$

in eq.(4), with an  $f(Q)$  that vanishes in the threshold  $f(m_h) = 0$ , and saturates to 1 for  $Q \gg m_h$  such as

$f(Q) = 1 - 2m_h/Q$ , would delay the onset of the massless-like behaviour, as shown for the charm contribution by the grey dotted lines in the upper panels of Fig.1, while

$$\hat{\sigma}_j^{\text{GM}} \longrightarrow \hat{\sigma}_j^{\text{GM}^*} = (1 - f(Q)) \hat{\sigma}_j^{\text{GM}} + f(Q) \hat{\sigma}_j^{\text{ZM}} \quad (8)$$

would suppress mass effects, as shown for the bottom contribution in the lower panels. In any case, it is clear that while the GM schemes introduce negligible corrections at the energy scale of the LEP experiments, mass effects are significant at the scales of Belle and BaBar. The remarkably precise measurements of the SIA cross section as a function of  $z$  performed by these experiments allows to check if a particular scheme is favored by the data.

*GMVFN scheme global analysis for FFs.*— In this section, we discuss the actual relevance of heavy quark mass corrections in charged pion production, implementing different factorization schemes in a NLO QCD global analysis for the extraction of FFs, performed along the lines of that of ref. [12]. The method for the global analysis has been described in detail in [3, 12]. It is based on an efficient Mellin moment technique that allows one to tabulate and store the computationally most demanding parts of the NLO calculation of SIA, SIDIS and proton-proton hadroproduction cross sections prior to the actual analysis. In this way, the evaluation of the relevant cross sections becomes so fast that can be easily performed inside a standard  $\chi^2$  minimization. At variance with [12], where SIA cross sections were evaluated only in the ZM approximation, here they are extended to the GM framework what requires to define different contours in the complex moment space to perform the Mellin inversion. Hadroproduction and SIDIS cross sections are still computed in the ZM framework, to asses in this first step the impact introduced by SIA corrections. Nevertheless, the heavy quark contributions to these processes are negligibly small. Also a minor difference with [12] is that we remove from the data sets included in the analysis TASSO and OPAL light flavor tagged data, that have comparatively large errors.

In Tab. I we compare the quality of a fit performed within the standard ZMVFN factorization scheme, and a GMVFN variant where the prescriptions of Eqs.(7) and (8) have been adopted for the charm and bottom coefficients respectively, as in the example of Fig.1. Among the different prescriptions we have explored, the above mentioned one reproduces best the data, significantly better than in the ZMVFN scheme, with much lower  $\chi_i^2$  values and smaller normalization shifts  $N_i$ . No significant improvement is found with more sophisticated weight functions  $f(Q)$ . On the other hand, the most simple subtraction of Eq.(5), produces fits of much poor quality, suggesting that such prescription oversubtracts for charm, and converges much slower to the massless limit than the data require for bottom.

As expected, heavy quark mass effects are most noticeable for Belle and Babar experiments, since at their relatively low center of mass energies heavy quarks are

TABLE I: Individual  $\chi^2$  values and normalization shifts  $N_i$  for the data sets included in global analyses where the ZMVFN and GMVFN schemes have been implemented.

| experiment    | data type        | # data in fit | ZMVFN |          | GMVFN |          |
|---------------|------------------|---------------|-------|----------|-------|----------|
|               |                  |               | $N_i$ | $\chi^2$ | $N_i$ | $\chi^2$ |
| ALEPH [23]    | incl.            | 22            | 0.968 | 21.6     | 0.994 | 23.3     |
| BABAR [13]    | incl.            | 39            | 1.019 | 76.7     | 1.002 | 58.2     |
| BELLE [14]    | incl.            | 78            | 1.044 | 19.5     | 1.019 | 11.0     |
| DELPHI [24]   | incl.            | 17            | 0.978 | 6.7      | 1.003 | 9.3      |
|               | <i>uds</i> tag   | 17            | 0.978 | 20.8     | 1.003 | 9.5      |
|               | <i>b</i> tag     | 17            | 0.978 | 10.5     | 1.003 | 7.8      |
| OPAL [25]     | incl.            | 21            | 0.946 | 27.9     | 0.970 | 15.9     |
| SLD [26]      | incl.            | 28            | 0.938 | 28.0     | 0.963 | 9.5      |
|               | <i>uds</i> tag   | 17            | 0.938 | 21.3     | 0.963 | 11.3     |
|               | <i>c</i> tag     | 17            | 0.938 | 34.0     | 0.963 | 19.8     |
|               | <i>b</i> tag     | 17            | 0.938 | 11.1     | 0.963 | 9.9      |
| TPC [27]      | incl.            | 17            | 0.997 | 31.7     | 1.006 | 27.9     |
|               | <i>uds</i> tag   | 9             | 0.997 | 2.0      | 1.006 | 2.0      |
|               | <i>c</i> tag     | 9             | 0.997 | 5.9      | 1.006 | 4.3      |
|               | <i>b</i> tag     | 9             | 0.997 | 9.6      | 1.006 | 10.9     |
| COMPASS [28]  | $\pi^\pm$ (d)    | 398           | 1.003 | 378.7    | 1.008 | 382.9    |
| HERMES [29]   | $\pi^\pm$ (p)    | 64            | 0.981 | 74.0     | 0.986 | 69.9     |
|               | $\pi^\pm$ (d)    | 64            | 0.980 | 107.3    | 0.985 | 103.7    |
| PHENIX [30]   | $\pi^0$          | 15            | 1.174 | 14.3     | 1.167 | 14.4     |
| STAR [31]     | $\pi^\pm, \pi^0$ | 38            | 1.205 | 31.2     | 1.202 | 33.8     |
| ALICE [32]    | $\pi^0$          | 11            | 0.696 | 33.3     | 0.700 | 31.2     |
| <b>TOTAL:</b> |                  | 924           |       | 966.4    |       | 875.8    |

far from behaving as massless. On the other hand, even though these experiments are above the bottom threshold  $2m_b$ , where the bottom should be considered as an active flavor in the ZMVFN scheme, the bottom is actually strongly suppressed, feature that is well accounted for in the GMVFN scheme. In Fig.2 we show the differences between the fit estimates and Belle and BaBar data, against the relative experimental error.

Notice that there is also a considerable improvement in the description of data from experiments at a higher energy scale. The difference between the massless and the mass dependent picture comes in this case from the

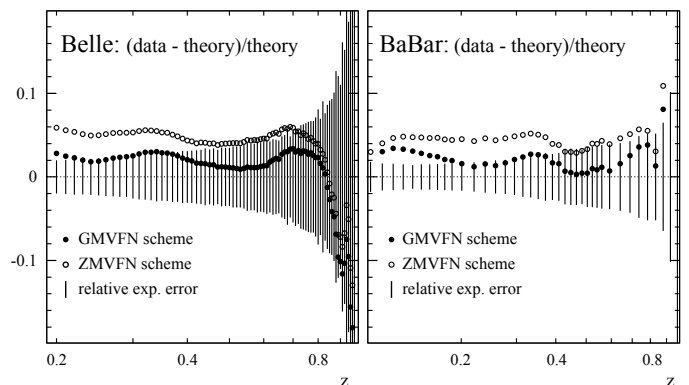


FIG. 2: Comparison between data from Belle and BaBar and estimates from the ZMVFN and GMVFN schemes

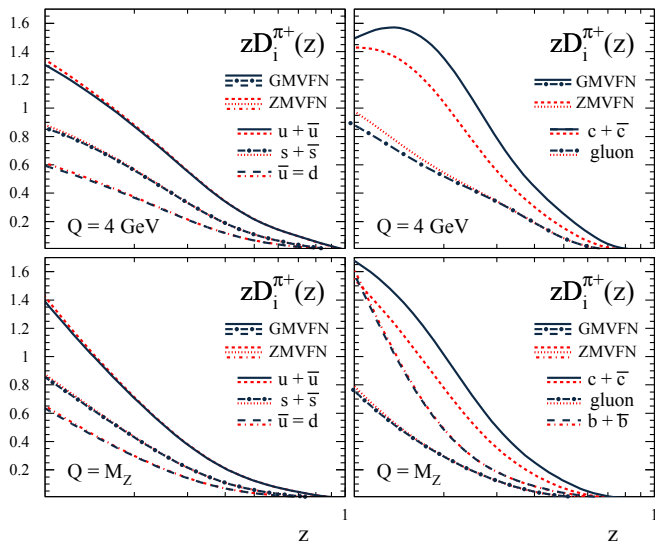


FIG. 3: FFs at  $Q = 4 \text{ GeV}$  and  $Q = M_Z$  coming from the ZMVFN and GMVFN schemes

fact that the QCD scale dependence preserves the difference between the charm fragmentation probabilities constrained by lower energy data, as shown in Fig.3. The bottom fragmentation probability is mainly constrained

by high energy flavor tagged SIA data, for which mass dependent corrections become negligible, and therefore the results for this flavor in both pictures agree. The GMVFN however guarantees that the bottom contribution at lower energies is conveniently suppressed, improving the overall agreement and consistency. No significant differences are found for the light flavors, that are constrained mainly by light flavor tagged SIA and SIDIS data.

*Conclusions and outlook.* — We have shown that an accurate determination of the fragmentation probabilities of quarks and gluons into pions, matching the precision of the present generation of hadroproduction experiments, requires a picture sensitive to heavy quarks dynamics. Such a picture was presented here, together with the results of a NLO QCD global analysis where it was implemented. Heavy quark mass dependence is specially relevant in single inclusive electron-positron annihilation into pions, where the detailed energy scale dependence of the charm contribution and the suppression of the bottom above their respective thresholds is non negligible. These effects are expected to be even more apparent in the production of heavy flavored mesons, where the mass dependent fragmentation probabilities are dominant.

We warmly acknowledge Daniel de Florian and Marco Stratmann for help and encouragement. This work was supported by CONICET, ANPCyT and UBACyT.

- 
- [1] See, e.g. R. D. Ball, M. Bonvini and L. Rottoli, JHEP **1511**, 122 (2015), and references therein.
- [2] For a review see, e.g. J. Rojo *et al.*, J. Phys. G **42**, 103103 (2015)
- [3] D. de Florian, R. Sassot and M. Stratmann, Phys. Rev. D **75**, 114010 (2007).
- [4] S. Albino, B. A. Kniehl, and G. Kramer, Nucl. Phys. B **725**, 181 (2005); *ibid.* **803**, 42 (2008); M. Hirai, S. Kumano, T. -H. Nagai, and K. Sudoh, Phys. Rev. D **75**, 094009 (2007).
- [5] M. A. G. Aivazis, J. C. Collins, F. I. Olness and W. K. Tung, Phys. Rev. D **50**, 3102 (1994)
- [6] R. S. Thorne and R. G. Roberts, Eur. Phys. J. C **19**, 339 (2001)
- [7] R. S. Thorne, Phys. Rev. D **73**, 054019 (2006).
- [8] M. Guzzi, P. M. Nadolsky, H. L. Lai and C.-P. Yuan, Phys. Rev. D **86**, 053005 (2012).
- [9] M. Cacciari, P. Nason and C. Oleari, JHEP **0510**, 034 (2005)
- [10] T. Kneesch, B. A. Kniehl, G. Kramer and I. Schienbein, Nucl. Phys. B **799**, 34 (2008)
- [11] B. A. Kniehl, G. Kramer, I. Schienbein and H. Spiesberger, Phys. Rev. D **77**, 014011 (2008).
- [12] D. de Florian, R. Sassot, M. Epele, R. J. Hernandez-Pinto and M. Stratmann, Phys. Rev. D **91**, no. 1, 014035 (2015).
- [13] J. P. Lees *et al.* [BABAR Collaboration], Phys. Rev. D **88**, 032011 (2013).
- [14] M. Leitgab *et al.* [BELLE Collaboration], Phys. Rev. Lett. **111**, 062002 (2013).
- [15] S. Forte, E. Laenen, P. Nason and J. Rojo, Nucl. Phys. B **834**, 116 (2010).
- [16] R. D. Ball *et al.* Phys. Lett. B **754**, 49 (2016)
- [17] G. Altarelli and G. Parisi, Nucl. Phys. B **126**, 298 (1977); Y. L. Dokshitzer, Sov. Phys. JETP **46**, 641 (1977) [Zh. Eksp. Teor. Fiz. **73**, 1216 (1977)]; V. N. Gribov and L. N. Lipatov, Sov. J. Nucl. Phys. **15**, 438 (1972).
- [18] G. Altarelli, R.K. Ellis, G. Martinelli, and S.Y. Pi, Nucl. Phys. **B160**, 301 (1979).
- [19] D. P. Anderle, F. Ringer and M. Stratmann, Phys. Rev. D **92**, no. 11, 114017 (2015).
- [20] J. C. Collins, Phys. Rev. D **58**, 094002 (1998)
- [21] M. Buza, Y. Matiounine, J. Smith and W. L. van Neerven, Eur. Phys. J. C **1**, 301 (1998).
- [22] B. A. Kniehl, G. Kramer, I. Schienbein and H. Spiesberger, Phys. Rev. D **71**, 014018 (2005); Eur. Phys. J. C **41**, 199 (2005).
- [23] D. Buskulic *et al.* [ALEPH Collaboration], Z. Phys. C **66**, 355 (1995).
- [24] P. Abreu *et al.* [DELPHI Collaboration], Eur. Phys. J. C **5**, 585 (1998).
- [25] R. Akers *et al.* [OPAL Collaboration], Z. Phys. C **63**, 181 (1994).
- [26] K. Abe *et al.* [SLD Collaboration], Phys. Rev. D **59**, 052001 (1999).
- [27] H. Aihara *et al.* [TPC/TWO GAMMA Collaboration], Phys. Lett. B **184**, 299 (1987); Phys. Rev. Lett. **61**, 1263 (1988).
- [28] N. Makke [COMPASS Collaboration], PoS DIS **2013**, 202 (2013).

- [29] A. Airapetian *et al.* [HERMES Collaboration], Phys. Rev. D **87**, 074029 (2013).
- [30] A. Adare *et al.* [PHENIX Collaboration], Phys. Rev. D **76**, 051106 (2007).
- [31] L. Adamczyk *et al.* [STAR Collaboration], Phys. Rev. D **89**, 012001 (2014).
- [32] B. Abelev *et al.* [ALICE Collaboration], Phys. Lett. B **717**, 162 (2012).